Experimental Analysis of Energy Transfers between a Quantum Emitter and Light Fields

I. Maillette de Buy Wenniger,[1] S. E. Thomas,[1] M. Maffei,[2] S. C. Wein,[2,3] M. Pont,[1] N. Belabas,[1] S. Prasad,[2] A. Harouri,[1] A. Lemaître,[1] I. Sagnes,[1] N. Somaschi,[3] A. Auffèves,[2,4,5,*] and P. Senellart[1,*]

[1]*Centre for Nanosciences and Nanotechnology, CNRS, Université Paris-Saclay, UMR 9001, 10 Boulevard Thomas Gobert, 91120 Palaiseau, France*

[2]*Université Grenoble Alpes, CNRS, Grenoble INP, Institut Néel, 38000 Grenoble, France*

[3]*Quandela SAS, 10 Boulevard Thomas Gobert, 91120 Palaiseau, France*

[4]*MajuLab, CNRS-UCA-SU-NUS-NTU International Joint Research Laboratory, Singapore, Singapore*

[5]*Centre for Quantum Technologies, National University of Singapore, 117543 Singapore, Singapore*

(Received 6 June 2023; revised 2 October 2023; accepted 14 November 2023; published 27 December 2023)

Energy can be transferred between two quantum systems in two forms: unitary energy—that can be used to drive another system—and correlation energy—that reflects past correlations. We propose and implement experimental protocols to access these energy transfers in interactions between a quantum emitter and light fields. Upon spontaneous emission, we measure the unitary energy transfer from the emitter to the light field and show that it never exceeds half the total energy transfer and is reduced when introducing decoherence. We then study the interference of the emitted field and a coherent laser field at a beam splitter and show that the nature of the energy transfer quantitatively depends on the quantum purity of the emitted field.

DOI: 10.1103/PhysRevLett.131.260401

Understanding and probing the nature of the energetic exchanges between quantum systems is of prime importance from both a fundamental and application point of view in the second quantum revolution. An emblematic textbook situation for quantum technologies is two coupled quantum systems that are otherwise isolated from their environment. For two quantum systems A and B, two different types of energy transfers can be identified. With the energy initially in A and subsequently fully transferred to B, we have at the end of the interaction $-\Delta\mathcal{E}_A = \Delta\mathcal{E}_B$. This allows one to define the unitary energy $E^{A,B}_{\text{unit}}$ as the energy transferred from A to B through an effective unitary interaction from the perspective of B. Such unitary energy can be associated with the notion of work for closed quantum systems [1–4] and results from a desirable process with no entropy increase. Such a framework is typical of single qubit gates, where the qubit remains in a pure state while exchanging energy with a driving field. This unitary energy can later be used to drive a third system and is limited by quantum correlations taking place during the interaction. The remaining energy, correlation energy $E^{A,B}_{\text{corr}} = \Delta\mathcal{E}_B - E^{A,B}_{\text{unit}}$, signals the presence of correlations or entanglement that occurred during the interaction. Being able to quantify and optimize these two types of energy is highly relevant to the field of quantum batteries [5–7], systems that can store energy from chargers and release it on demand. It also carries the seeds for the macroscopic analysis of the energetic cost of quantum information processing [8–11].

Experimentally exploring these questions is very challenging: it requires simultaneously the ability to accurately access energy changes in each quantum system and their correlations (i.e., respecting global energy conservation), and to trace back how these systems exchanged energy. So far, experiments have mostly focused on energy changes experienced by only one (open) quantum system, e.g., polarized photons [12], ions [13], nuclear spins [14], or on average energy exchanges between two systems [8,15]. Here, we take a leap forward, by proposing and implementing experimental protocols to access the unitary and correlation energies exchanged in a closed bipartite system in two scenarios [Figs. 1(a) and 1(b)]: the spontaneous emission of a quantum emitter, and the interference between the emitted field and a coherent laser field. The emitter is a semiconductor quantum dot weakly coupled to an optical microcavity. We experimentally access the unitary energy emitted during spontaneous emission by performing self-homodyne measurements with the emitted light field. At low temperature, we measure that the unitary energy represents almost 50% of the total energy transferred from the emitter to the field, close to the theoretical limit [16]. By increasing the emitter temperature we study the impact of pure dephasing, and observe a reduction of

the unitary energy evidencing loss of coherence induced by the environment of the emitter. In the second scenario, we probe energetic exchanges between the emitted field and a laser field by interfering them on a beam splitter. The unitary energy transferred is shown to be limited by the purity of the quantum field and the relative coherence of both fields.

The first energy transfer that we study involves a qubit (q) coupled to a reservoir of electromagnetic modes. At the initial time, the qubit is resonantly excited by a laser drive and brought into the pure quantum superposition state $|\Psi_q\rangle = \cos(\theta/2)|g\rangle + \sin(\theta/2)e^{i\alpha}|e\rangle$, with $|g\rangle$ and $|e\rangle$ ground and excited states separated by energy $\hbar\omega_0$, and θ, α the pulse area and the classical phase of the driving laser, respectively. The initial energy brought to the emitter is $\mathcal{E}_q = \hbar\omega_0 \sin^2(\theta/2)$. After spontaneous emission, this energy is entirely transferred to the electromagnetic field (f): $\Delta\mathcal{E}_{q,f} = \mathcal{E}_q$. In the absence of decoherence, the emitted field state is pure and reads as $|\Psi_f\rangle = \cos(\theta/2)|0\rangle + \sin(\theta/2)e^{i\alpha}|1\rangle$, where $|0\rangle$ and $|1\rangle$ are the photon-number states with populations $p_0 = \cos^2(\theta/2)$ and $p_1 = \sin^2(\theta/2)$; see Fig. 1(a). The unitary energy transferred to the field corresponds to the coherent part of the emitted field energy [16,17] and reads as $E^{q,f}_{\text{unit}} = \hbar\omega_0 s^2$, where s is the coherence of the qubit before spontaneous emission: $s = \cos(\theta/2)\sin(\theta/2)$. The fraction of unitary energy is thus maximal at $\theta = \pi/2$ and amounts to 50% of the initial energy. Conversely, the correlation energy, $E^{q,f}_{\text{corr}} = \Delta\mathcal{E}_{q,f} - E^{q,f}_{\text{unit}}$, corresponds to the incoherent component of the emitted field, and is maximal for $\theta = \pi$ where all the energy is transferred in the form of correlation energy.

We experimentally probe these energy processes with an InGaAs quantum dot (QD) coupled to a micropillar cavity [18,19]. The system operates in the weak coupling regime where the QD is effectively coupled to a one-dimensional continuum of optical modes. At a temperature of 5 K, these artificial atoms have been shown to be close to textbook qubit systems with negligible influence of the solid-state environment, attested to by the generation of single photons with near-unity indistinguishability [19]. In 2019, they remarkably allowed for the first demonstration in the optical domain that a coherently driven qubit emits wave packets in a quantum superposition of $|0\rangle$ and $|1\rangle$ [20]. The QD in a cryostation is resonantly driven by 7 ps laser pulses at 925 nm using a Ti:sapphire laser operating at an 81 MHz repetition rate [Fig. 1(c)]. The emitted photonic field is separated from the laser drive using a cross-polarization configuration. Black symbols in Fig. 2(a) correspond to the normalized intensity μ_f of the emitted field as a function of pulse area θ of the driving laser. The onset of Rabi oscillations attests for coherent control over the qubit, i.e., the ability to generate arbitrary quantum superpositions of the qubit ground and excited state. We assume a near-unity occupation of the qubit excited state at power P_π corresponding to maximum emission intensity such that $\theta = 2\arcsin(\sqrt{P/P_\pi})$ (Fig. S1). This experimental curve then corresponds to the normalized energy of the emitted field $\Delta\mathcal{E}_{q,f}/(\hbar\omega_0) = \mu_f = \sin^2(\theta/2)$ (black line).

We experimentally measure the unitary energy transfers during spontaneous emission by performing self-homodyne measurements with the emitted field. In the absence of decoherence, we show that the resulting visibility of interference v directly corresponds to the unitary energy divided by the total energy, $v = E^{q,f}_{\text{unit}}/\Delta\mathcal{E}_{q,f} = \cos^2(\theta/2)$ (see the Supplemental Material [21]). This energy fraction can be interpreted as the efficiency of the process aimed at solely transferring unitary energy. As shown in configuration 1 of Fig. 1(c), using a flip mirror we temporally overlap two

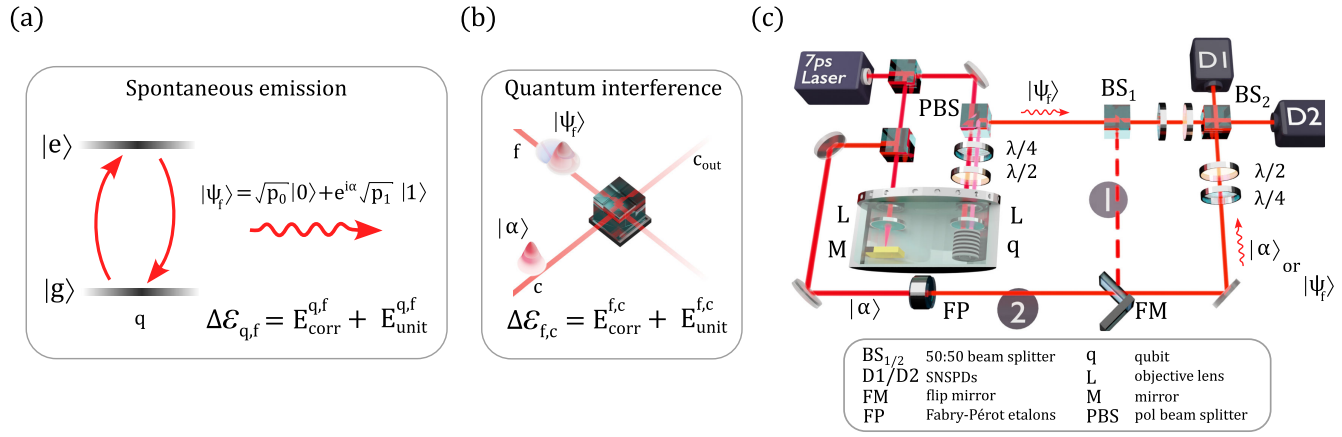

FIG. 1. Measuring energetic transfers. (a) The first scenario studied. Energetic transfers in spontaneous emission, from a quantum emitter "q" to the vacuum of the electromagnetic field "f." (b) The second scenario studied. Energetic transfers from the spontaneously emitted field to a coherent laser field "c" at a beam splitter. (c) Experimental implementation showing configurations 1 and 2, depending on the scenario studied. In both configurations, the output intensities are recorded using two superconducting nanowire single-photon detectors $D1$ and $D2$. See main text for details.

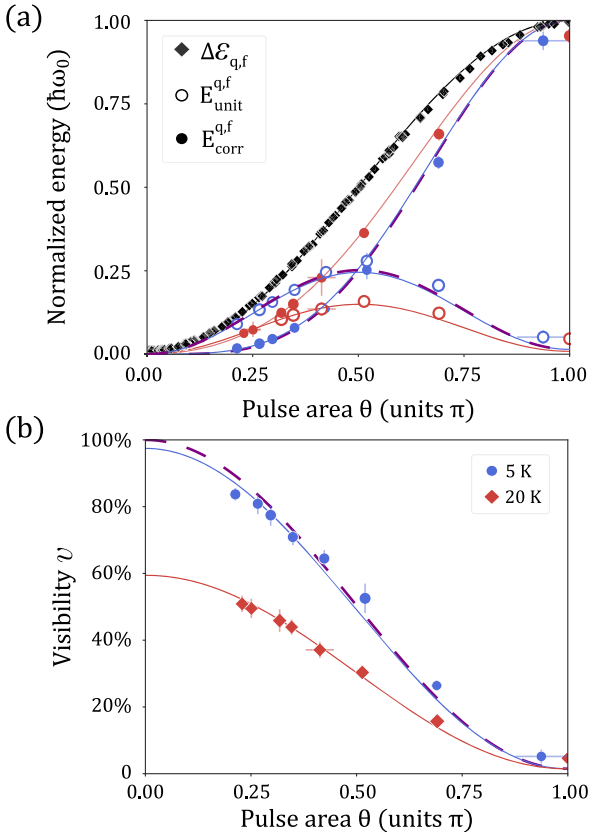

FIG. 2. Energy transfer during spontaneous emission. (a) Total energy transferred from the qubit "q" to the vacuum of the electromagnetic field "f" $\Delta\mathcal{E}_{q,f}$ (diamonds), unitary energy $E^{q,f}_{\mathrm{unit}}$ (open circles), and correlation energy $E^{q,f}_{\mathrm{corr}}$ (filled circles) as a function of pulse area θ. (b) Measured visibility v of the photonic field. Blue (red) symbols correspond to measurements at 5 K (20 K). Dashed lines (purple) correspond to theory without any decoherence. The red and blue lines correspond to theory considering pure dephasing, with corrections accounting for imperfect laser rejection.

successively emitted fields separated by 12.5 ns at beam splitter BS_2. With two single-photon detectors we record the intensities, which show anticorrelated oscillations as a function of the relative phase ϕ between two interfering fields [20], and extract the interference visibility v.

Figure 2(b) shows v as a function of θ: it decreases continuously with increasing θ, as theoretically expected. We can deduce the amount of unitary energy $E^{q,f}_{\mathrm{unit}} = \Delta\mathcal{E}_{q,f} \times v$. Figure 2(a) displays $E^{q,f}_{\mathrm{unit}}$ in units of $\hbar\omega_0$ as a function of θ (open symbols), and the corresponding correlation energy $E^{q,f}_{\mathrm{corr}} = \Delta\mathcal{E}_{q,f} \times (1 - v)$ (filled symbols) and the theoretical predictions without decoherence (dashed lines). Our observations at 5 K are close to the theoretical predictions [16]. At low θ, most of the energy transferred is of unitary nature. Indeed, in the low excitation regime, the radiated field stems from the qubit dipole: no light-matter entanglement takes place, and the emitted field is remarkably close to a coherent field. Conversely, light-matter entanglement builds up when a qubit population is created. Although at the end of spontaneous emission the qubit and field are in a separable state, quantum correlations taking place during spontaneous emission reduce the amount of unitary energy transferred to the electromagnetic field, with only correlation energy transferred in the limit $\theta \to \pi$. In this situation, the emitted field contains no coherent component. The unitary energy transfer is maximal for $\theta = \pi/2$, with an equipartition of unitary and correlation energy. This corresponds to maximal initial coherence in the qubit state.

We now investigate how pure dephasing impacts the transfer of the quantum coherence imprinted between the ground and excited state of the emitter onto the emitted field, by increasing the temperature of the QD. At 20 K, the phonon sideband is strongly suppressed by the Purcell effect induced by the cavity [25], and the qubit is mostly subject to phonon-induced pure dephasing. Although the quantum emitter does not exchange energy with the phonon reservoir, both interact, and correlations are created between them. We extend our theoretical framework to include phonon coupling and show that the unitary energy still equals the coherent energy of the emitted field (see the Supplemental Material [21]). This emitted field is now described by the density matrix $\hat{\rho}_f = \cos^2(\theta/2)\hat{\rho}_0 + \sin^2(\theta/2)\hat{\rho}_1 + \cos(\theta/2)\sin(\theta/2)(\hat{\rho}_{01} + \hat{\rho}_{10})$ where the subscripts 0 and 1 represent the vacuum and one-photon part of the field, respectively. $M_{\mathrm{s}} = \mathrm{Tr}[\hat{\rho}_1^2]$ is the single-photon indistinguishability or purity of the single-photon component in the temporal domain [26]. The reduction of quantum coherence between the vacuum and the one-photon component is captured by $\mathcal{C} = \mathrm{Tr}[\hat{\rho}_{01}\hat{\rho}_{10}]$. The unitary energy provided by the qubit to the field reads as $E^{q,f}_{\mathrm{unit}} = \hbar\omega_0\mathcal{C}\cos^2(\theta/2)\sin^2(\theta/2)$. Notably, our study shows that in the case of pure dephasing, the unitary energy is limited by the photon indistinguishability through $\mathcal{C} = M_{\mathrm{s}}$ (see the Supplemental Material [21]).

Figure 2(b) shows the visibility of the self-homodyne measurement at 20 K, evidencing unitary energy transfer between the QD and the optical field. The efficiency is reduced compared with 5 K. We fit both datasets and find $\mathcal{C}(5\ \mathrm{K}) = 0.975 \pm 0.007$ and $\mathcal{C}(20\ \mathrm{K}) = 0.594 \pm 0.007$. This is consistent with the independently measured single-photon indistinguishability $M_{\mathrm{s}}(5\ \mathrm{K}) = (92.6 \pm 0.1)\%$, and $M_{\mathrm{s}}(20\ \mathrm{K}) = (58.0 \pm 1.0)\%$. The unitary energy remains maximal for $\theta = \pi/2$, but its value has reduced from $E^{q,f}_{\mathrm{unit}}/\hbar\omega_0 = (27.9 \pm 1.2)\%$ at 5 K to $E^{q,f}_{\mathrm{unit}}/\hbar\omega_0 = (15.8 \pm 0.6)\%$ at 20 K. Our observations reveal how probing the nature of energy exchanges between quantum systems provides access to their past correlations. At 5 K where the two systems are isolated, the correlation energy carries information on past entanglement even if both systems are not entangled anymore. At 20 K, where the qubit is also coupled to a pure dephasing environment, it allows one to

identify if unwanted correlations with an environment built up during interaction.

In a second step, we study the energetic exchanges between the emitted field (f) and a coherent laser field (c), hereafter called the "classical" field, coupled through a 50:50 beam splitter [Fig. 1(b)]. Such configuration is instrumental to induce effective light-light interaction in optical quantum technologies. The emitted field can be seen as a drive for the classical field, transferring unitary and correlation energy to the latter. We extended our theoretical framework to capture this new situation. We demonstrate that for such a beam-splitter-induced interaction, the unitary energy received by a light field equals the change of its coherent energy (see the Supplemental Material [21]). Experimentally, we set the input energies of both fields to be equal to maximize the interference visibility v, i.e., $\mathcal{E}_f^{\text{in}} = \mathcal{E}_{\text{c}}^{\text{in}} = \hbar\omega_0 \sin^2(\theta/2)$, and consider one of the outputs as hosting the resulting field, c_{out}. Now the interference visibility v provides access to the total energy exchanged (see the Supplemental Material [21]). The energy transferred to the classical field reads as $\Delta\mathcal{E}_{f,\text{c}} = \mathcal{E}_f^{\text{in}} \times v$, with $v = 1$ signaling complete transfer. The visibility is given by $v = \mathcal{C}_{f,\text{c}} \cos(\theta/2)$ where $\mathcal{C}_{f,\text{c}}$ quantifies the overall classical and quantum coherence between both fields. If the QD is initially subject to pure dephasing, we show that $\mathcal{C}_{f,\text{c}} = M_{f,\text{c}}$, where $M_{f,\text{c}}$ is the mean wave packet overlap between the quantum and the classical field (see the Supplemental Material [21]).

We find that the correlation energy is dictated by the quantum field (see the Supplemental Material [21]): $E_{\text{corr}}^{f,\text{c}} = E_{\text{corr}}^{q,f}/2$ which reflects the fact that only the quantum field carries an incoherent component. We can thus deduce the unitary energy component using $E_{\text{unit}}^{f,\text{c}} = \mathcal{E}_f^{\text{in}} \times v - E_{\text{corr}}^{q,f}/2$, which is upper bounded by the unitary energy initially given to the quantum field: $E_{\text{unit}}^{q,f} \geq E_{\text{unit}}^{f,\text{c}}$ (see the Supplemental Material [21]). This demonstrates that only the unitary energy received by the emitted field in the first scenario can be used to drive the classical field through the beam splitter in the second scenario. Figure 3(a) presents the theory curves for the unitary, correlation, and total energy transfers in the ideal situation of a pure quantum state. Once again, most of the energy is transferred in the form of unitary energy in the limit where $\theta \to 0$, i.e., when the state of the quantum field is closest to the classical field and the energy transfer is complete. $\Delta\mathcal{E}_{f,\text{c}}$ is maximum for $\pi/2 < \theta < \pi$, a behavior that results from a trade-off between maximum quantum field coherence at $\theta = \pi/2$ and the coherence of the classical field continuously increasing with θ. For large θ, the unitary energy becomes negative, signaling flow of unitary energy in the opposite direction: from the classical field to the quantum field. Finally, when $\theta = \pi$ the quantum field consists of a single-photon pulse, giving rise to maximum correlation energy input of half a photon into the classical field. No interference takes place; hence, no energy is transferred to the classical field. In this situation, correlation and unitary energy cancel out.

We experimentally study this interference both at 5 K and 20 K using configuration 2 in Fig. 1(c). To minimize the effect of vibrations in our closed-cycle cryostation, the classical field is sent into the same cryostation and focused by an objective lens (L) onto a mirror. To further increase the signal-to-noise ratio, the classical field is spectrally shaped using Fabry-Pérot etalons (FP) to increase its temporal overlap with the quantum field (Fig. S3). Using detectors $D1$ and $D2$, we observe phase-dependent oscillations in counts from which we extract the interference visibility plotted as a function of pulse area θ in Fig. 3(b). As theoretically predicted, an increasing visibility is observed when reducing θ, both at 5 K and 20 K, evidencing energy transfer toward the classical field of

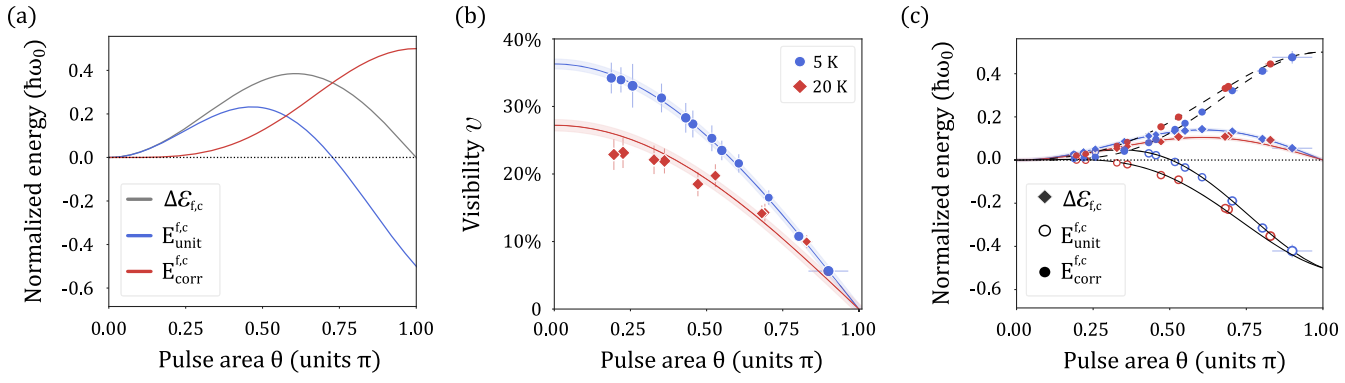

FIG. 3. Energy exchanges in quantum interference. (a) The theoretical total energy, unitary, and correlation energy transfers from the photonic field "f" to the coherent laser field "c" in the ideal case. (b) Measured visibility v as a function of θ (blue 5 K, red 20 K). The solid lines are a theoretical fit to the data using $v = \cos(\theta/2)\mathcal{C}_{f,\text{c}}$, and the shaded regions represent 2σ uncertainty in the fit. (c) Measured total energy $\Delta\mathcal{E}_{f,\text{c}}$, the correlation energy $E_{\text{corr}}^{f,\text{c}}$, and the unitary energy $E_{\text{unit}}^{f,\text{c}}$ transferred from the quantum field to the coherent laser field as a function of θ. Lines correspond to theoretical fits with deduced parameters $\mathcal{C}_{f,\text{c}}$ and $\mathcal{C}$.

increasing efficiency. Our observations are well reproduced by $v = \Delta\mathcal{E}_{f,c}/\mathcal{E}_f^{in} = \cos(\theta/2)\mathcal{C}_{f,c}$ for $\mathcal{C}_{f,c}(5\text{ K}) = (36.3 \pm 0.4)\%$ and $\mathcal{C}_{f,c}(20\text{ K}) = (27.2 \pm 0.4)\%$.

Figure 3(c) shows the unitary, correlation, and total energy transfers deduced from the visibility measured in Fig. 3(b) and the measurement of the correlation energy received by the quantum field deduced from Fig. 2(b). While the energy transfer during spontaneous emission at 5 K was close to the ideal case, this second step deviates from theoretical maximum with significantly reduced maximum energy exchanged, and positive unitary energy flows for a smaller θ range. The situation is even worse at 20 K, where the unitary energy flows in the opposite direction for most of the θ range.

To understand these observations, we measured the mean wave packet overlaps between the quantum field and the classical field. We find $M_{f,c}(5\text{ K}) = (48.9 \pm 0.3)\%$ and $M_{f,c}(20\text{ K}) = (32.3 \pm 0.7)\%$. Overall, the expected upper bound of $\mathcal{C}_{f,c} = M_{f,c}$ is not reached, an observation that is probably due to residual blinking of the QD transition that results in an unbalanced interference and affects differently the measurements of $\mathcal{C}_{f,c}$ (from single counts) and $M_{f,c}$ (from coincidence counts). Note that this is in contrast with the first experiment based on a self-homodyne measurement where blinking impacts both inputs simultaneously and thus maintains the interference balance.

In conclusion, we proposed and implemented experimental protocols to measure the unitary and correlation energy exchanged between a two-level system and the electromagnetic field, and between two optical fields. The two experimental situations studied here constitute key building blocks for a multitude of quantum technologies from atom-based quantum memories, linear optical gates to Bell state measurements among others. In particular, quantum superpositions of 0 and 1 photon are important resources for quantum communications such as twin-field protocols [27] that have so far been implemented with attenuated coherent fields only. As such, the second part of our work constitutes an experimental milestone toward higher security by exploiting a true quantum field, while providing insight into the energetics of quantum communication schemes harnessing Fock state superpositions. Finally, the present work is highly relevant in the field of quantum batteries. In this framework, the quantum dot represents a work provider and the electromagnetic modes at the output of the device a quantum battery. Here the first step of our protocol corresponds to charging of the battery and the second to its discharge into a classical field. By measuring the unitary energy transfer, we quantify the energy that can later be used to drive another system. In both steps, we evidenced the importance of the classical and quantum coherence on the unitary energy transfers.

We acknowledge financial support by the Agence Nationale de la Recherche (QuDICE project), the H2020-FET OPEN Project No. 899544—PHOQUSING, the French RENATECH network, the Paris Ile-de-France Region in the framework of DIM SIRTEQ, the Foundational Questions Institute Fund (Grant No. FQXi-IAF19-05), the Templeton World Charity Foundation, Inc. (Grant No. TWCF0338).

*Correspondence and requests for data should be addressed to A. A. (alexia.auffeves@cnrs.fr) and P. S. (pascale.senellart-mardon@c2n.upsaclay.fr).

[1] S. Alipour, F. Benatti, F. Bakhshinezhad, M. Afsary, S. Marcantoni, and A. T. Rezakhani, Sci. Rep. **6**, 35568 (2016).
[2] H. Hossein-Nejad, E. J. O'Reilly, and A. Olaya-Castro, New J. Phys. **17**, 075014 (2015).
[3] H. Weimer, M. J. Henrich, F. Rempp, H. Schröder, and G. Mahler, Europhys. Lett. **83**, 30008 (2008).
[4] H. Schröder and G. Mahler, Phys. Rev. E **81**, 021118 (2010).
[5] J. Quach, K. Mcghee, L. Ganzer, D. Rouse, B. Lovett, E. Gauger, J. Keeling, G. Cerullo, D. Lidzey, and T. Virgili, Sci. Adv. **8**, eabk3160 (2022).
[6] F. C. Binder, S. Vinjanampathy, K. Modi, and J. Goold, New J. Phys. **17**, 075015 (2015).
[7] G. M. Andolina, M. Keck, A. Mari, M. Campisi, V. Giovannetti, and M. Polini, Phys. Rev. Lett. **122**, 047702 (2019).
[8] J. Stevens, D. Szombati, M. Maffei, C. Elouard, R. Assouly, N. Cottet, R. Dassonneville, Q. Ficheux, S. Zeppetzauer, A. Bienfait, A. N. Jordan, A. Auffèves, and B. Huard, Phys. Rev. Lett. **129**, 110601 (2022).
[9] J. Gea-Banacloche, Phys. Rev. Lett. **89**, 217901 (2002).
[10] M. Ozawa, Phys. Rev. Lett. **89**, 057902 (2002).
[11] A. Auffèves, PRX Quantum **3**, 020101 (2022).
[12] V. Cimini, S. Gherardini, M. Barbieri, I. Gianani, M. Sbroscia, L. Buffoni, M. Paternostro, and F. Caruso, npj Quantum Inf. **6**, 96 (2020).
[13] D. Von Lindenfels, O. Gräb, C. T. Schmiegelow, V. Kaushal, J. Schulz, M. T. Mitchison, J. Goold, F. Schmidt-Kaler, and U. G. Poschinger, Phys. Rev. Lett. **123**, 080602 (2019).
[14] J. P. S. Peterson, T. B. Batalhão, M. Herrera, A. M. Souza, R. S. Sarthour, I. S. Oliveira, and R. M. Serra, Phys. Rev. Lett. **123**, 240601 (2019).
[15] N. Cottet, S. Jezouin, L. Bretheau, P. Campagne-Ibarcq, Q. Ficheux, J. Anders, A. Auffèves, R. Azouit, P. Rouchon, and B. Huard, Proc. Natl. Acad. Sci. U.S.A. **114**, 7561 (2017).
[16] J. Monsel, M. Fellous-Asiani, B. Huard, and A. Auffèves, Phys. Rev. Lett. **124**, 130601 (2020).
[17] M. Maffei, P. A. Camati, and A. Auffèves, Phys. Rev. Res. **3**, L032073 (2021).
[18] V. Giesz, N. Somaschi, G. Hornecker, T. Grange, B. Reznychenko, L. D. Santis, J. Demory, C. Gomez, I. Sagnes, A. Lemaître, O. Krebs, N. D. Lanzillotti-Kimura, L. Lanco, A. Auffeves, and P. Senellart, Nat. Commun. **7**, 11986 (2016).
[19] N. Somaschi, V. Giesz, L. De Santis, J. C. Loredo, M. P. Almeida, G. Hornecker, S. L. Portalupi, T. Grange, C. Antón, J. Demory, C. Gómez, I. Sagnes, N. D. Lanzillotti-Kimura,

A. Lemaítre, A. Auffeves, A. G. White, L. Lanco, and P. Senellart, Nat. Photonics **10**, 340 (2016).
[20] J. C. Loredo, C. Antón, B. Reznychenko, P. Hilaire, A. Harouri, C. Millet, H. Ollivier, N. Somaschi, L. De Santis, A. Lemaître, I. Sagnes, L. Lanco, A. Auffèves, O. Krebs, and P. Senellart, Nat. Photonics **13**, 803 (2019).
[21] See Supplemental Material at http://link.aps.org/supplemental/10.1103/PhysRevLett.131.260401 for theoretical analysis and experimental procedures, which includes Refs. [22–24].
[22] Ş. K. Özdemir, A. Miranowicz, M. Koashi, and N. Imoto, Phys. Rev. A **66**, 053809 (2002).
[23] H. Ollivier, S. E. Thomas, S. C. Wein, I. Maillette de Buy Wenniger, N. Coste, J. Loredo, N. Somaschi, A. Harouri, A. Lemaitre, I. Sagnes *et al.*, Phys. Rev. Lett. **126**, 063602 (2021).
[24] S. C. Wein, J. C. Loredo, M. Maffei, P. Hilaire, A. Harouri, N. Somaschi, A. Lemaître, I. Sagnes, L. Lanco, O. Krebs, A. Auffèves, C. Simon, P. Senellart, and C. Antón-Solanas, Nat. Photonics **16**, 374 (2022).
[25] T. Grange, N. Somaschi, C. Antón, L. De Santis, G. Coppola, V. Giesz, A. Lemaître, I. Sagnes, A. Auffèves, and P. Senellart, Phys. Rev. Lett. **118**, 253602 (2017).
[26] C. Santori, D. Fattal, J. Vučković, G. S. Solomon, and Y. Yamamoto, Nature (London) **419**, 594 (2002).
[27] M. Lucamarini, Z. L. Yuan, J. F. Dynes, and A. J. Shields, Nature (London) **557**, 400 (2018).